

SPARE GUN MULTI-PHYSICS ANALYSIS FOR LCLS-II*

L. Xiao[†], C. Adolphsen, A. Cedillo, E. Jongewaard, X. Liu, C.-K. Ng, F. Zhou
SLAC National Accelerator Laboratory, Menlo Park, CA 94025, USA

Abstract

LBNL APEX VHF normal conducting (NC) gun was adopted for LCLS-II continuous wave (CW) operation to provide ultra-bright high repetition rate X-ray pulses. The initial LCLS-II gun and injector commissioning showed excessive dark current dominated by field emission. There is a concern that the dark current may get worse with time of operation. It is planning to build a spare gun for LCLS-II to replace the existing one. The proposed spare gun design largely based on the current LCLS-II gun has a reduced peak electrical field by 10%. In addition, there are some moderate modifications on the spare gun engineering design and fabrication plan to increase mechanical robustness and in-vacuum performance. SLAC developed parallel finite-element electromagnetic code suite ACE3P is used to apply for the spare gun modelling including RF, thermal and structural analysis to ensure its successful operation in LCLS-II. In this paper, the spare gun multi-physics analysis is described.

INTRODUCTION

A modified LBNL APEX gun as shown in Fig. 1 has been installed in LCLS-II injector [1]. The initial LCLS-II gun and injector commissioning results showed excessive dark current dominated by field emission around the cathode plug outer diameter and the gun cavity nose near the gap [2, 3].

LBNL has proposed a new design largely based on the existing LCLS-II gun as shown in Fig. 2 [4]. The elliptical shapes instead of the circler ones in LCLS-II gun at the corners of the cathode gap, anode nose and cavity nose cone have been carefully optimized in the new gun design, which has a 10% lower of the peak electrical fields. The LBNL new gun design is planned to be built as a spare gun for LCLS-II to replace the existing one. The RF parameters in the spare gun and the exist LCLS-II gun are listed in Table 1, where E_c and E_s represent the electrical fields on the cathode centre and the cavity wall.

The spare gun engineering design utilizes the existing LCLS-II gun model as much as possible. There are some moderate changes for the affected regions due to the cavity geometry changes and other improvements. The spare gun and the existing LCLS-II gun mechanical models are shown in Fig.3. The end cap has a reduced inner radius for similar structural support as LCLS-II gun. The bucking coil is moved upstream 2 mm to increase the wall thickness at the cavity nose for better thermal path. The thicker cavity wall cooling tube is used for the robustness of in-vacuum performance. Two stainless steel (SS) inserts are added in the cavity and anode noses for dark current reduction. The

fundamental power couplers in the existing LCLS-II gun and the spare gun are the same, which are not included in the simulations.

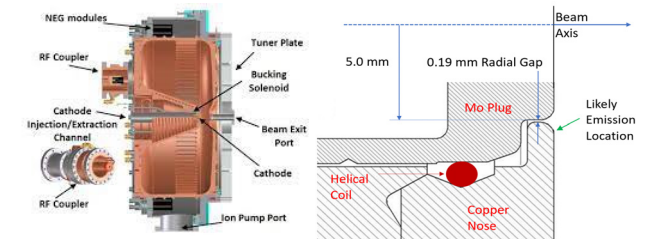


Figure 1: LCLS-II gun CAD model (left) and the drawing around the cathode gap (right). Courtesy of LBNL.

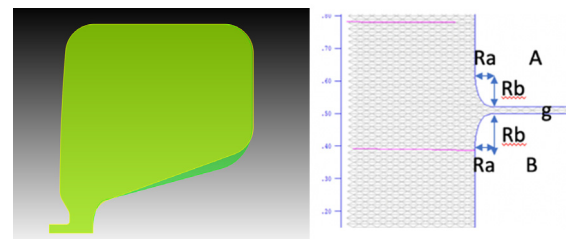


Figure 2: The cavity shapes of LCLS-II spare gun (in green) and the existing gun (in yellow) (left) and the geometry shape of the spare gun cathode plug (right). Courtesy of LBNL T. Luo.

Table 1: The RF Parameters in the Spare Gun and the Existing LCLS-II Gun

Peak Electrical Field	Spare Gun	LCLS-II Gun
	($R_a = 0.25$ mm, $R_b = 1.5$ mm, $g = 0.2$ mm)	($R_a = R_b = 1.0$ mm, $g = 0.19$ mm)
Peak E_s/E_c	1.10	1.24
Peak E_A/E_c	1.06	1.19
Peak E_B/E_c	1.06	1.22

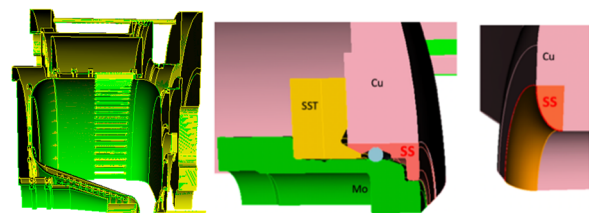


Figure 3: The multi-physics simulation models of LCLS-II spare gun (in green) and the existing gun (in yellow) (left), and the spare gun CAD model around the two SS inserts (right).

APEX gun multi-physics simulations have been done using commercial software packages such as ANSYS and CST [5, 6]. In this paper, the spare gun multi-physics simulations are carried out using ACE3P codes [7]. Running on the National Energy Research Scientific Computing

* Work supported by US DOE under contract AC02-76SF00515.

[†] lilting@slac.stanford.edu

Center (NERSC) supercomputer for high fidelity and high accuracy simulations [8], ACE3P codes enable rapid running time with sufficient details in the spare gun multi-physics analysis to ensure the reliability of the spare gun operation in LCLS-II injector. ACE3P codes have been applied for many accelerator projects [9]. In this paper the spare gun RF, thermal and structural analysis for LCLS-II is presented. Multipacting analysis as well as field enhancement study due to the cathode plug misalignment are discussed.

SPARE GUN MULTI-PHYSICS ANALYSIS

The spare gun multi-physics analysis starts with the RF field calculation for the operating mode at 184 MHz using the electromagnetic eigensolver Omega3P. The wall loss induced by the magnetic field scaled with 20 MV/m of the electrical field at the cathode center is applied as the heat flux load on the surface boundary between the cavity vacuum and metal regions. The temperature distribution from the thermal solver in TEM3P is calculated in the cavity wall. The deformation and the stress fields on the cavity body due to the changes in the temperature field are calculated from the elastic solver in TEM3P. The spare gun RF, thermal and structural results are shown in Fig. 4.

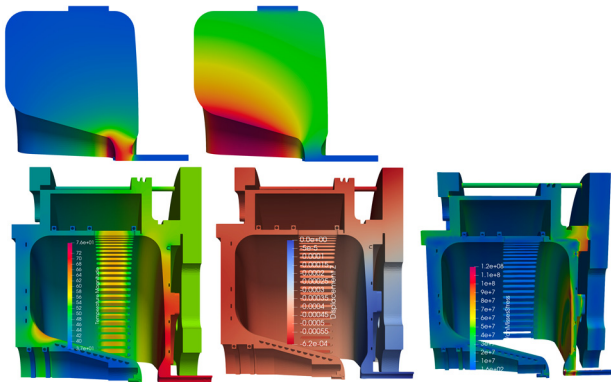


Figure 4: The spare gun electrical (upper left) and magnetic fields (upper right), temperature ($^{\circ}\text{C}$) (down left), displacement z-component (m) (down middle) and von Mises (Pa) (down right) distributions with $E_c = 20 \text{ MV/m}$.

The material properties and the cooling water parameters used in the simulations are listed in Tables 2 and 3, respectively. The end of the beampipe serves as the reference point in the mechanical simulations and the two symmetry planes have the symmetry constraints. The room temperature is 30°C .

The maximum temperature is 76°C located on the SS anode nose, 5°C higher than the one using copper material. The maximum SS stress is $1.0 \times 10^8 \text{ Pa}$, well below its yield strength.

The deformed cavity body due to the RF thermal expansion is shown in Fig. 5 by scaling 50 times larger for visualization. The eigenmode in the deformed cavity closure is recalculated using Omega3P and the RF frequency increases by 150 kHz, which is 50 kHz lower than the

existing LCLS-II gun. The gun cavity has vacuumed inside, and thus the air pressure outside the cavity enclosure can cause the cavity deformation as well. Simulations show that the frequency can decrease by around 120 kHz in both the spare gun and the existing LCLS-II gun due to the air pressure.

Table 2: The Material Properties

	K (W/m. $^{\circ}\text{C}$)	G (N/m 2)	μ (N/m 2)	α (1/ $^{\circ}\text{C}$)	σ (s/m)
Cu	391	4.51e10	7.16e10	1.77e-5	5.8e7
Al	150	2.78e10	5.03e10	2.36e-5	-
Mo	138	1.22e11	1.92e11	4.8e-6	1.8e7
SS	14	7.51e10	1.24e11	1.73e-6	1.4e6

Table 3: The Cooling Water Parameters

Water Inlet T = 30°C	T ($^{\circ}\text{C}$)	H (W/m 2 . $^{\circ}\text{C}$)			
Cavity Wall	35	1.54e4			
Anode 1 2 3 4	42	6790	6560	5710	5730
Cavity Nose Cone	35	2.99e4			
Cathode 1 2 3 4	35	1.96e4	2.03e4	2.37e4	
			2.52e4		

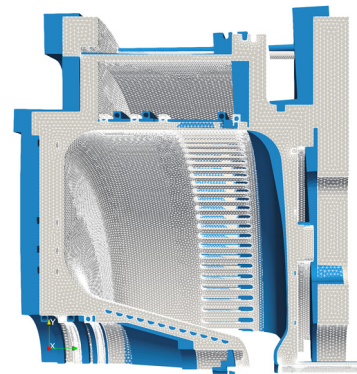


Figure 5: The spare gun cavity bodies before (meshed in grey) and after (in blue) the thermal expansion due to the RF load.

Table 4: The Spare Gun and the Existing LCLS-II Gun Thermal and Structural Simulations Results

$E_c = 20 \text{ MV/m}$	Spare Gun	LCLS-II Gun
DF (KHz)	150	184
Max. T ($^{\circ}\text{C}$)	76	73
Cu Power Loss (W)	87e3	91e3
Mo Power Loss (W)	0.2	0.1
SS Power Loss (W)	21	-

Both the simulation results for the spare gun and the existing LCLS-II gun are listed in Table 4. The spare gun thermal and structural performance are acceptable.

SPARE GUN MULTIPACTING SIMULATIONS

To have multipacting (MP) in the spare gun cavity, electrons must be resonant with the RF fields and can be multiplied via secondary electron emission. The resonant particles are searched from 25 kV/m to 20 MV/m for the electrical field at the cathode center using the particle tracking code Track3P. The resonant particles in the spare gun and the existing LCLS-II gun are plotted in Fig. 6. There are no new resonant particles found in the spare gun.

Possible MP is located on the cavity wall corner at the anode side for the cathode field between 3 MV/m to 9 MV/m. At lower field levels such as 3 MV/m to 6 MV/m at the cathode center, secondary electrons are emitted at impacts, but the synchronization with RF fields takes many RF cycles as shown in Fig. 7. The MP barrier can be considered as soft. At higher field levels, the resonant particles have very high impact energy and are not likely to have secondary emission. We expect that the MP in the spare gun can be processed through as the existing LCLS-II gun.

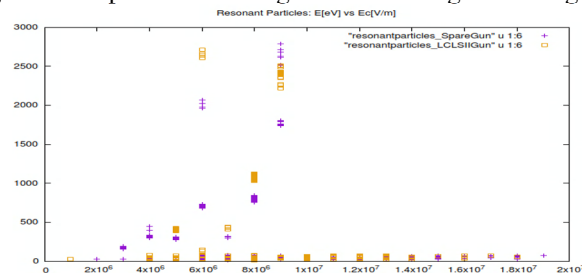


Figure 6: The resonant particle impact energy versus the electric field at the cathode center.

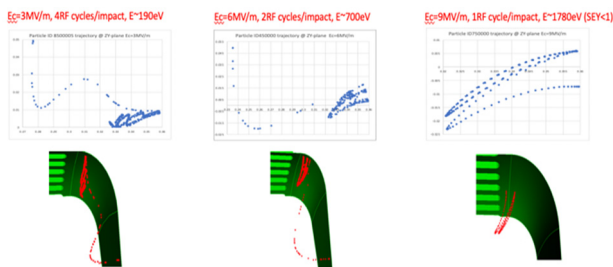


Figure 7: The resonant particle trajectories in the spare gun with 3 MV/m (left), 6 MV/m (middle) and 9 MV/m (right) of the electric field at the cathode center.

SPATRE GUN CATHODE PLUG MISALIGNMENT STUDY

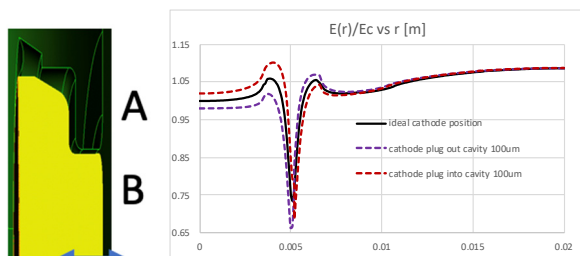


Figure 8: The CAD model of the cathode plug (left) and the electric field distributions on the cathode and cavity nose flat surfaces (right).

There is local electric field enhancement due to the cathode plug misalignment. The spare gun shape is optimized having the same peak electric field at the cathode plug gap regions A and B as shown in Fig. 8 when the cathode plug is flushed with the cavity nose flat surface. When the cathode plug misalignment along the beam direction is within 100 μm , there is 5% of field enhancement. The field enhancement due to the cathode offset from the center is not noticeable.

SUMMARY

The spare gun multi-physics analysis has been performed using ACE3P codes. The spare gun thermal and mechanical performances are acceptable. Next we plan to perform the spare gun cavity multi-physics modeling by adding the power couplers and with more details. The recently implemented time-domain thermal solver in TEM3P will be used to simulate the spare gun RF transient effect [10]. The spare gun multi-physics modeling has a typical 2.2M tetrahedral elements, corresponding to about 7M degrees of freedom in solving a linear system of equations. The run time was 40 minutes using 640 compute cores on NERSC Cori supercomputer, demonstrating the efficient performance of ACE3P's parallel computation.

ACKNOWLEDGEMENTS

This research used resources of the National Energy Research Scientific Computing Center (NERSC), a U.S. Department of Energy Office of Science User Facility operated under Contract No. DE-AC02-05CH11231.

REFERENCES

- [1] F. Sannibale *et al.*, “Advanced photoinjector experiment photogun commission results”, *Phys. Rev. Spec. Top.-Ac.*, vol. 15, p. 103501, 2012.
doi:10.1103/PhysRevSTAB.15.103501
- [2] J. F. Schmerge *et al.*, “The LCLS-II Injector Design”, in *Proc. Of 36th Int. Free Electron Laser Conf. (FEL'2014)*, Basel, Switzerland, Aug. 2014, paper THP042, pp. 815-819.
- [3] F. Zhou *et al.*, “First Commissioning of LCLS-II CW Injector Source”, in *Proc. Of 10th Int. Particle Accelerator Conf. (IPAC'2019)*, Melbourne, Australia, May 2019, pp. 2171-2173. doi:10.18429/JACoW-IPAC2019-TUPTS106
- [4] T. Luo, H. Feng, and D. Li, “LCLS-II Spare Gun Preliminary RF Study”, presented at the 2020 Virtual SSRL/LCLS Users' Meeting, Sept. 2020.
- [5] R. P. Wells *et al.*, “Mechanical design and fabrication of the VHF-Gun, the Berkeley normal-conducting continuous-wave high-brightness electron source”, *Review of Scientific Instruments*, vol. 87, no. 2, p. 023302, 2016.
doi:10.1063/1.4941836
- [6] G. Shu, Y. Chen, S. Lal, H. J. Qian, H. Shaker, and F. Stephan, “Multiphysics Analysis of a CW VHF Gun for European XFEL”, in *Proc. 39th Int. Free Electron Laser Conf. (FEL'19)*, Hamburg, Germany, Aug. 2019, pp. 456-459. doi:10.18429/JACoW-FEL2019-WEP055

- [7] Materials for CW18,
[https://confluence.slac.stanford.edu/
display/AdvComp/Materials+for+CW18](https://confluence.slac.stanford.edu/display/AdvComp/Materials+for+CW18)
- [8] Scientific Discovery through Advanced Computing,
<https://www.scidac.gov/>
- [9] L. Xiao, L. Ge, Z. Li, and C.-K. Ng, “Advances in Multiphysics Modelling for Parallel Finite-Element Code Suite ACE3P”, *IEEE J. Multiscale Multiphysics Comput. Tech.*, vol. 4, pp. 298–306, 2019,
doi:10.1109/JMMCT.2019.2954946
- [10] C.-K. Ng, L. Ge, Z. Li, and L. Xiao, “A Parallel Time Domain Thermal Solver for Transient Analysis of Accelerator Cavities”, presented at the 12th Int. Particle Accelerator Conf. (IPAC’21), Campinas, Brazil, May 2021, paper TUPAB248, this conference.